Heliyon 10 (2024) e35750

Contents lists available at ScienceDirect

Heliyon

journal homepage: www.cell.com/heliyon

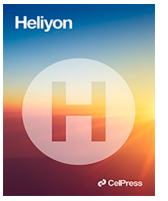

Research article

Electroacupuncture improves retinal function in myopia Guinea pigs probably via inhibition of the RhoA/ROCK2 signaling pathway

Yijie Liu [a], Qi Hao [a], Xiuzhen Lu [b], Pubo Wang [a], Dadong Guo [b], Xiuyan Zhang [b], Xuemei Pan [b], Qiuxin Wu [b,**], Hongsheng Bi [b,*]

[a] *Shandong University of Traditional Chinese Medicine, Jinan, Shandong Province, 250014, China*
[b] *Affiliated Eye Hospital of Shandong University of Traditional Chinese Medicine, Shandong Academy of Eye Disease Prevention and Therapy, Shandong Provincial Key Laboratory of Integrated Traditional Chinese and Western Medicine for Prevention and Therapy of Ocular Diseases, Jinan, Shandong Province, 250002, China*

ARTICLE INFO

Keywords:
Myopia
electroacupuncture
Retina
Ras homologous gene-Rho-associated coiled-coil forming kinase(Rho-ROCK) signaling pathway

ABSTRACT

Objective: To investigate the effect of electroacupuncture (EA) on retinal function in guinea pigs with negative lens-induced myopia (LIM) by inhibiting the RhoA/ROCK2 signaling pathway.
Methods: Guinea pigs were randomly divided into normal control (NC) group, LIM group, EA group, SHAM acupoint (SHAM) group, and electro-acupuncture + ROCK pathway inhibitor Y27632 (EA + Y27632) group. The refraction, axial length, retinal blood flow density, choroidal vascular index, retinal physiological function, the contents of total antioxidant capacity (T-AOC), catalase (CAT), glutathione (GSH), superoxide dismutase (SOD) and malondialdehyde (MDA) of each group were determined. The changes in retinal tissue structure were observed by hematoxylin and eosin (H&E) staining, and the expression of the RhoA/ROCK2 signaling pathway-related molecules in the retina was measured by real-time quantitative polymerase chain reaction (qPCR) and Western blot.
Results: Myopic refraction, AL, and MDA content in the LIM and SHAM groups were significantly increased, retinal blood flow density and CVI, SOD, GSH, CAT, T-AOC content were decreased. After EA intervention, myopic refraction, AL, and MDA content decreased, retinal blood flow density and CVI, SOD, GSH, CAT, T-AOC content were increased. H&E staining showed that the thickness of the guinea pig retina, the thickness of the inner and outer layers of the nucleus, and the number of cells were significantly increased after EA intervention. qPCR and western blot analyses showed that the expression of RhoA、ROCK2、MLC、CollagenI、MMP-2、TIMP-2 and α-SMA were elevated in the LIM and SHAM group than those in the NC group. Compared with the LIM group, the expression of EA group was significantly decreased.
Conclusions: Electroacupuncture can improve retinal function by improving retinal blood flow, reducing retinal oxidative damage, inhibiting RhoA/ROCK2 signaling pathway and controlling extracellular matrix remodeling, thus delaying the occurrence and development of myopia.

* Corresponding author.
** Corresponding author.
E-mail addresses: wuqiuxin@163.com (Q. Wu), hongshengbi1@163.com (H. Bi).

https://doi.org/10.1016/j.heliyon.2024.e35750
Received 27 May 2024; Received in revised form 2 August 2024; Accepted 2 August 2024
Available online 5 August 2024

1. Introduction

Myopia is rapidly increasing at an alarming rate, which makes it a worldwide public health problem. Currently, myopia patients account for about 28.3 % of the global population, which is expected to increase to 49.8 % by 2050 [1]. The situation is even more serious in China, where the myopia rate among children and adolescents has reached 53.6 % in 2018 and is expected to increase to 84 % by 2050, according to the National Health Commission [2]. Myopia not only affects visual quality, but also increases the risk of various ocular diseases such as retinal detachment, choroidal neovascularization, macular degeneration, and glaucoma as myopia deepens. Therefore, actively controlling and intervening in the development of myopia is currently the focus of international research and one of the major issues facing the medical community.

As the first station for perceiving visual signals, the retina plays an important role in the etiology of myopia. The retina is a fine-layered structure with numerous cells that process complex visual signals through multiple molecular pathways. The dopaminergic mechanism, contribution of rods and cones photoreceptors, and structural changes in the retinal pigment epithelium (RPE) and neuroretinal layer in myopia all suggest that retinal dysfunction plays a crucial role in the development of myopia [3]. However, the specific mechanisms of the retina in the development of myopia are not yet clear.

Compared to normal eyes, myopic eyes exhibit reduced retinal vascular density, insufficient blood flow in the choroidal capillary layer [4], and decreased choroidal blood flow, which subsequently affects oxygen supply. Tissue hypoxia and insufficient blood supply can promote fibroblast differentiation into myofibroblasts, leading to extracellular matrix (ECM) remodeling [5]. The ECM is a microenvironment that cells rely on [6]. Hypoxia and oxidative stress are key regulators of ECM remodeling [7] as well as important causes of myopia, and reducing oxidative stress can help slow down myopia progression [8].

The Rho/ROCK signaling pathway is a ubiquitous signal transduction pathway in various tissues in vivo, which is involved in diverse physiological functions such as cytoskeletal recombination, cell migration, vascular and tissue permeability, tissue contraction and growth. The Rho protein belongs to the Ras superfamily of small GTPase molecules with GTPase activity, and the RhoA subtype has been extensively investigated [9].

ROCK, also known as Rho-associated coiled-coil kinase, is a serine/threonine protein kinase and serves as the key downstream effector molecule of Rho. Studies have demonstrated that the Rho/ROCK signaling pathway can regulate intraocular vascular smooth muscle contraction, participate in intraocular blood flow regulation, and modulate choroidal angiogenesis [10]. ROCK inhibitors exert vasodilatory effects on conjunctival blood vessels [11] and ciliary arteries [12], improve retinal microcirculation [13] and enhance ocular blood flow. Additionally, they can inhibit proliferation, migration, and angiogenesis of vascular endothelial cells [14–16]. Moreover, the inhibitory effect of ROCK can prevent neuronal damage by protecting the retina from excitotoxicity while promoting axon growth [17,18]. However, the mechanism of underlying Rho/ROCK signaling in the retina remains unclear.

Acupuncture has been widely utilized for treating various diseases due to its safety profile and proven efficacy. Acupuncture demonstrates promising effectiveness in preventing myopia, however, the molecular mechanisms underlying its impact on myopic retina remain poorly understood. In this study, our objective was to investigate the impact of EA on myopia and elucidate its mechanism of action by establishing a LIM guinea pig model and exploring the role of the Rho/ROCK signaling pathway in the retina of LIM guinea pigs. Additionally,we aimed to clarify whether EA can enhance retinal function and inhibit myopia development by modulating the Rho/ROCK signaling pathway. Our study provides a theoretical foundation for utilizing EA in the prevention and management of myopia, as well as novel insights for addressing myopia in adolescents.

2. Materials and methods

2.1. Animals

The study was approved by the Experimental Animal Ethics Review Committee of Affiliated Hospital of Shandong University of Traditional Chinese Medicine (Approval number: AWE-2022-055) and followed the Association for Research in Vision and Ophthalmology (ARVO) guidelines for animal use in vision research. Healthy two-week-old guinea pigs (Cavia porcellus, British Shorthair, Tricolor strain, Jinan Jinfeng Laboratory Animal Company, Jinan, China) with a mass of 110 ± 10 g were used for the entire experiment. Before enrollment, ocular parameters were measured to exclude ocular diseases such as cataracts or ocular fundus lesions. Subsequently, the eligible guinea pigs were randomly divided into normal control (NC) group, lens-induced myopia (LIM) group, electro-acupuncture (EA) group, SHAM acupoint (SHAM) group, and electro-acupuncture + ROCK pathway inhibitor Y27632 (EA + Y27632) group. The guinea pigs were kept in the animal room of the Institute of Ophthalmology, Shandong University of Traditional Chinese Medicine. The room temperature was kept at 25 °C, the circadian rhythm was controlled for 12/12h, and the guinea pigs were fed freely.

2.2. Experimental myopic induction and electroacupuncture treatment

The NC group did not receive any intervention. LIM group, EA group, SHAM group, and EA + Y27632 group wore a −6.0D lens in the right eye and no lens in the left eye. Inspect twice every morning and evening to observe the mental state and glasses-wearing of guinea pigs. If there is any abnormality, deal with it in time to avoid affecting the modeling.

EA group and EA + Y27632 group were given electrical stimulation with continuous wave, intensity 2 mA, pulse length 0.1s, frequency 2HZ by electronic needle therapy apparatus. Acupoint selection: On both sides of the Taiyang (EX-HN5) point (posterior temporal fossa of the outer corner of the eye, slanted 2 ~ 3 mm down the subcutaneous side) and Hegu (IL4) point (between the first

and second metacarpal bones of the forelimb, directly stabbed 3 mm) [19]. The SHAM group stimulated both sides of the buttocks away from the traditional meridians. Once a day, 30 min each time, the time is fixed at 9:00 a.m. to 12:00 a.m. Y27632 was applied to the right eye three times a day at a concentration of 10 mM. The experiment contents and time points were shown in Fig. 1.

2.3. Biometric Measurement

1 % cyclopentolate hydrochloride eye drops (Alcon, Geneva, Switzerland) were used for cycloplegia, 5 min/time for 4 consecutive times, and 30 min later the examination was performed.

Streak retinoscope (Suzhou 66 Vision Technology Co., Ltd, China) for refractive examination was used to determine the refraction parameters. Streak retinoscope screening was performed in a dark room with a working distance of 50 cm and the average of the two principal meridians, horizontal and vertical, was taken as the final refractive value. Two eyes were measured at least three times, and the average value was the final experimental result.

The AL was determined by A-scan ultrasonography (CineScan, Quantel Medical, France). According to the reference, [20] the A-scan ultrasonography was set: the propagation velocities in the anterior chamber, vitreous cavity and lens were 1557 m/s, 1540 m/s and 1723 m/s, respectively. The eye surface was anesthetized with 1 % obucaine hydrochloride eye drops (Benoxicam, Japan) before the A-scan ultrasonography measurement. About 3 min after anesthesia, the center of the probe was aligned with the vertex of the guinea pigs'cornea for measurement, and the average value was taken for 10 consecutive measurements. All of the above procedures are performed by the same professional ophthalmologist.

2.4. Flash visual evoked potential (F-VEP)

In the present study, we used an ophthalmic imaging system (OPTO-III, UK) to perform F-VEP detection. The guinea pigs were anesthetized and fixed on the experimental operating platform (the heating system was used to maintain a constant body temperature). Before the experiment, the guinea pigs were fully acclimated to darkness for 2 h, their eyes were fully dilated with 1 % cyclopentolate hydrochloride eye drops (Alcon, Geneva, Switzerland), and Sodium pentobarbital (50 ml/kg) was injected into the abdomen for anesthesia. The F-VEP recording electrode was inserted into the skin of the guinea pig at the midpoint of the connection between the ear edges, 0.5 cm behind the fontanel. Each guinea pig elicited an N–P–N waveform. When one eye is stimulated, the other eye is covered with a homemade black eye mask. In this study, only P2 latency and peak were recorded. VEP parameter setting: magnification 40K, stimulation frequency 1.0Hz, stimulation light intensity 3.0 cd s/m^2.

2.5. Retinal flash electroretinography (F-ERG)

The preparation before inspection is the same as F-VEP. The electrodes were placed in a dark red light and sodium hyaluronate eye drops were applied to keep the cornea moist. The reference electrode was inserted into the lower lip, the ground electrode was inserted into the corresponding forelimb, and the F-ERG recording electrode was placed in the cornea of both eyes. After the above steps were completed, the dark adaptation ERG was detected in sequence, and the bright adaptation ERG was recorded after 10 min of bright adaptation (under 30 cd s/m^2 background light). According to international standardization requirements [21], and then F-ERG

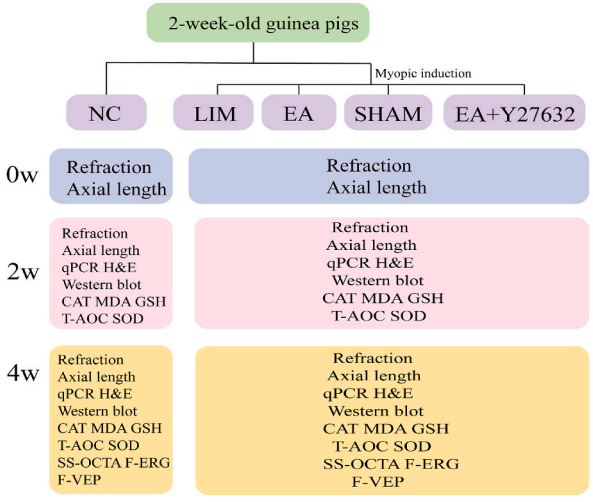

Fig. 1. Experimental flow chart. NC: Normal control; LIM: Lens-induced myopia; EA: Electroacupuncture; SHAM: Sham acupoint; T-AOC: total antioxidant capacity; CAT; catalase; GSH: glutathione; SOD: superoxide dismutase; MDA: malondialdehyde; H&E: hematoxylin and eosin; qPCR = real-time quantitative PCR; FERG = flash electroretinogram; F-VEP: Flash visual evoked potential; SS-OCTA; Swept-Source Optical Coherence Tomography Angiography.

measurements were performed and recorded. The F-ERG recording contents and parameter settings are shown in Table 1 below.

2.6. SS-OCTA

The choroidal vascularity index (CVI) and retinal blood flow density was measured by using wide-field Swept-Source Optical Coherence Tomography Angiography (SS-OCTA) (TowardPi BMizar, TowardPi Medical Technology, Beijing, China) and analyzed with custom-made software. Choroidal vascular volume (CVV) is the volume of the choroidal Sattler's middle vascular layer and Haller's large vessel layer. CVI indicates the ratio of lumen area (LA) to total choroidal area (TCA), which reflects the choroidal vascular density of the middle vascular layer of the Sattler and the large vessel layer of the Haller, and the higher the CVI is, the greater the ratio of the vascular tissues in the choroid and the more blood flow is abundant [22]. In addition, we calculated the choroidal stromal index (CSI) by subtracting the CVI from 1 (CSI = 1 - CVI). The above parameters were measured automatically by an artificial intelligence-based algorithm.

At 4 weeks after modeling, OCTA was performed under cycloplegia. One person fixed the guinea pig in the appropriate position of the OCT jaw frame, and the other person scanned the posterior pole of the guinea pig's eye according to the method of using the device. Each eye was measured three times. The images were divided into 9 quadrants using a 3 × 3 grid, and the image with the optic disc in the center quadrant, the highest image resolution, and the least amount of data loss was selected for further analysis(Fig. 2A–C). If the software's automatic segmentation was incorrect, manual segmentation was performed based on the judgment of an independent examiner, and the software automatically calculated the average blood flow density in each region.

2.7. Detection of SOD, GSH, CAT, MDA content and total antioxidant capacity (T-AOC)

Two and four weeks after molding, retina tissues from guinea pigs were extracted and frozen in liquid nitrogen. Tissues were accurately weighed, and 10 % tissue homogenate was made by adding 9 times of saline according to the ratio of weight (g): volume (ml) = 1:9, centrifuged at 2500 rpm for 10 min, and the supernatant was taken to determine the contents of superoxide dismutase (SOD), glutathione (GSH), catalase (CAT), malondialdehyde (MDA) and the total antioxidant capacity (T-AOC). In this study, BCA protein assay kit (Beyotime Biotechnology, China) was used to detect the protein concentration of tissue homogenate, and the contents of SOD, GSH, CAT, MDA, and T-AOC were detected and calculated according to the instruction manual of each kit (Nanjing Jiancheng Bioengineering Institute, China). Three replicates were set up in each group.

2.8. Real-time fluorescent quantitative PCR

Two and four weeks after molding, retina tissues from guinea pigs were extracted and frozen in liquid nitrogen. Then, equal amounts of retina tissues were taken and ground separately using a modified tissue/cellular RNA rapid extraction kit (SparkJade Science Co., Ltd., Jinan, China) to extract total RNA. The RNA purity and concentration were measured by an ultraviolet spectrophotometer (K5600; Beijing Kaiao Technology Development Co., Ltd., Beijing, China). The HiScript II Q RT SuperMix for qPCR (+gDNA wiper) (Vazyme Biotech Co., Ltd., Nanjing, China)was used for reverse transcription. The 96-well plates (NEST Biotechnology, Wuxi, China) were used for real-time quantitative PCR (qPCR) to determine the levels of Rhoa, Rock2, myosin light chain (MLC), tissue inhibitor of metalloproteinase-2 (TIMP-2), matrix metalloproteinase 2 (MMP2), α-sma, and Collagen I with the 96-well plates (NEST Biotechnology, Wuxi, China). The primer sequences were listed in Table 2. The qPCR conditions were as follows: 94 °C for 5 s, 1 cycle; 94 °C for 5 s, 54 °C for 15 s, and 72 °C for 10 s for 45 cycles. The expres-sion level of the target gene in each sample was normalized to the internal reference level of glyceraldehyde 3-phosphate dehydrogenase (GAPDH), and the result was analyzed using the $2^{-\triangle\triangle Ct}$ method [23].

2.9. Western blot analysis

To investigate the protein levels of the molecules related to the RhoA/ROCK2 signaling pathway, we used western blot assays to determine the RhoA、ROCK2、MLC、p-MLC、CollagenI、MMP-2、TIMP-2 and α- SMA protein levels. After 2 and 4 weeks of mold making, the retinal tissue was separated, and PMSF and RIPA were added at the mass volume ratio of 10 mg:100 μL, then fully blown

Table 1
F-ERG records and parameter Settings.

Check item	Background light	Flash stimulation	Stimulus light intensity(cd·s/m^2)	Flash stimulation time (ms)
Dark adaptation				
Dark adapted rod cell response(Rod-ERG)	No	Single white	0.01	5
Dark adaptation maximal mixed response(Max-ERG)	No	Single white	3.0	5
Dark-adapted oscillatory potential(OPs-ERG)	No	Single white	3.0	5
Light adaptation				
Clearly adapted cone cell response(Cone-ERG)	30cd/m^2Intensity light	Single white	3.0	5

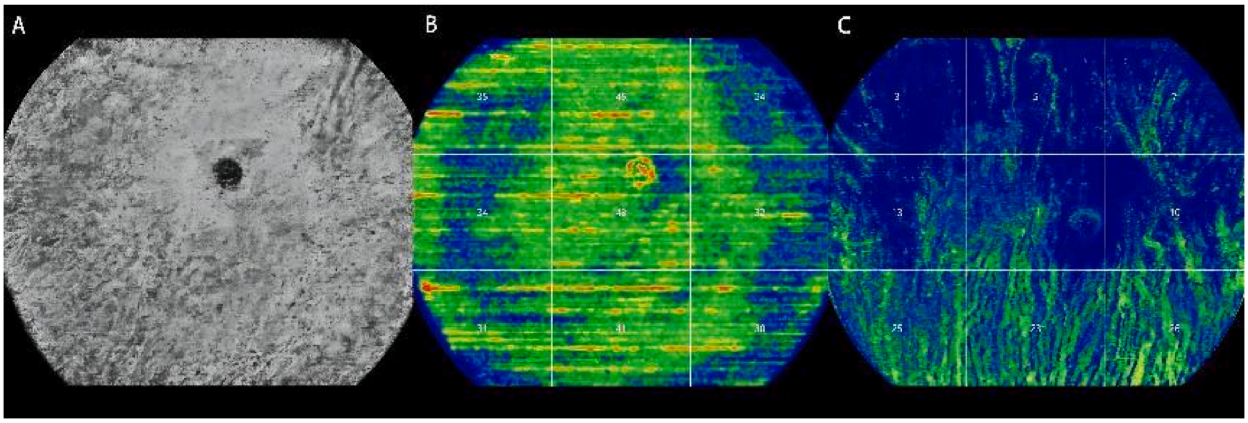

Fig. 2. SS-OCTA images. A Image of the choroidal capillary layer. **B** Image of retinal blood flow density. **C** Image of blood flow density in the middle and large vessel layers of the choroid. Using a 3 × 3 grid to divide the image into 9 quadrants, the image with the optic disc in the center quadrant, the highest image resolution, and the least amount of data loss was selected and automatically analyzed by the software. The blue portion indicates that this location is thin and has a low blood flow density.

Table 2
Primer sequence of the target genes.

Gene		Primer Sequences(5′-3′)
GAPDH	Forward	TCAAGAAGGTGGTGAAGCAGG
	Reverse	CTGTTGCTGTAGCCGAACTCAT
Rhoa	Forward	GCTGCCATCCGAAAGAAACT
	Reverse	GTGTCCCACAAAGCCAACTCT
Rock2	Forward	CACAAGGACCACTTAGACAGAAAGG
	Reverse	TCTTCACCAGGCGGCTCAC
mlc	Forward	CTCCGGGCACTGGGCACAAATC
	Reverse	TCAAAGACGCGCAGACCCTCAACA
collagen I	Forward	CAAGTTGTGGACCAAGACAGAGAC
	Reverse	CCTTACAGGTCATCTCTTCGCAC
mmp-2	Forward	GATGCCTTTGCTCGAGCCTT
	Reverse	GCCCATCCTTCCCATCGAAC
timp-2	Forward	TGTCGGTGGGAAGAAGGAATATC
	Reverse	TCTGGGTGGTACTCAGGGTGTC
α-sma	Forward	TTCAACGTCCCAGCCATGTATGTG
	Reverse	GTGACACCATCGCCAGAATCCAG

and mixed, electric homogenized for 6 min, centrifuged at 5000 rpm for 5 min, and the supe rserum was taken into the new sterile EP tube. Ultrasonic crushing was carried out under ice bath conditions for 10 min (working for 15 s, suspended for 10 s), and centrifugation at 5000 rpm for 5 min. The concentration of the supernatant of each sample was determined using a BCA protein concentration assay kit (Beyotime Biotechnology, Shanghai, China). The target proteins were then separated by electrophoresis on 10 % sodium dodecyl sulfate-polyacrylamide gels (SDS-PAGE) and then transferred to poly-vinylidene difluoride (PVDF) for blotting. The β-actin (Wuhan Xavier Biotechnology Co, Ltd., Wuhan, China), Collagen I (dilution 1:500; Bioss, Beijing, China), MLC(dilution1:500; Bioss, Beijing, China), p-MLC(dilution1:500; CST, USA), RhoA (dilution1:500; abcam, Shanghai, China), Rock2 (dilution1:500; Bioss, Beijing, China), MMP-2 (dilution1:500; NOVUS, USA), TIMP-2(dilution1:500; NOVUS, USA), α- SMA(dilution 1:500; Bioss, Beijing, China), primary the PVDF membranes loaded with target proteins were then incubated with secondary anti-bodies (dilution 1:10,000; Bioss, Beijing, China) for 1 h at room temperature. After washing, the blots were allowed to react with enhanced chemiluminescence (ECL) solutions (Millipore Corporation, Billerica, MA01821, USA) and exposed to ECL Hyperfilm (Vilber Lourmat Lourmat, Marne-la-Vallee, France). The relative protein amount (the ratio of the target protein gray value to the internal reference protein gray value) of each group was calculated and compared. In order to facilitate comparison, we normalized each group, and the mean of the NC group of the same period was 1. The experiment was repeated at least 3 times. The relative intensity of each band was determined using a computerized software program.

2.10. Histopathological staining

Two and four weeks later, 1 % Sodium pentobarbital was over-injected intraperitoneally, and the guinea pig eyeballs were removed, rinsed in sterile normal saline, and periocular tissue was removed, immediately placed in eyeball fixation solution for 24 h, and then routine dehydration, paraffin embedding and section were performed. Hematoxylin-eosin (H & E) staining was performed to

observe the physiological morphological and structural changes of the retina of each guinea pig's model eye.

2.11. Statistical analysis

SPSS21.0 statistical software was used to analyze the data, data were expressed in Mean ± SD, one-way ANOVA was used for comparisons between multiple groups, LSD-t-test for inter-group comparisons, and independent samples *t*-test for two-way comparisons between groups, and $P < 0.05$ was considered statistically significant difference.

3. Results

3.1. Effects of EA on refraction in LIM Guinea pigs

There was no significant difference in diopter between the groups before modeling. After 2 and 4 weeks of modeling, the myopia diopter of the LIM group was significantly increased compared with the NC group ($P < 0.05$; Table .3); The myopia diopter of EA and EA + Y27632 groups was decreased compared with the LIM group, and the difference was statistically significant ($P < 0.05$). There was no significant difference in diopter between the SHAM group and LIM group ($P > 0.05$). The diopter changes in the LIM group indicated that the myopia model was successfully induced and the diopter increased after the guinea pigs were given right eyeglasses for 2 and 4 weeks, while the myopia diopter decreased after the EA intervention, indicating that EA could effectively delay the development of myopia in LIM guinea pigs.

3.2. Effects of EA on axial length in LIM Guinea pigs

There was no statistically significant difference in axial length between the groups before modeling. After 2 and 4 weeks of modeling, the LIM group showed a significant increase in axial length compared with the NC group ($P < 0.05$, Table 4), the EA and EA + Y27632 groups showed a significant decrease in axial length compared with the LIM group ($P < 0.05$), and the difference in axial length between the LIM group and the SHAM group was not statistically significant ($P > 0.05$). It indicates that EA can effectively control the growth of the eye axis in LIM guinea pigs.

3.3. Effects of EA on F-ERG and F-VEP in LIM Guinea pigs

F-ERG results (Figs. 3 and 4 A-B) showed that compared with the NC group, there was no significant difference in latency between dark adaptation and light adaptation in the LIM group ($P > 0.05$), and the peak value was significantly reduced ($P < 0.05$). Compared with the LIM group, there was no obvious difference in latency of dark adaptation and light adaptation in the EA group and EA + Y27632 group ($P > 0.05$), and the peak values were significantly increased ($P < 0.05$).

F-VEP results (Figs. 3 and 4 A-B) showed that there was no significant difference in P2 latency among the groups. Compared with the LIM group, the peak value of P2 in the EA group and the EA + Y27632 group increased, and the difference was statistically significant ($P < 0.05$).

These results suggest that EA can improve the retinal function of LIM guinea pigs by increasing the peak values of F-ERG and F-VEP.

3.4. SS-OCTA images

After 4 weeks of modeling, the mean retinal blood flow density, CVI, and CVV were significantly lower in the LIM group compared with the NC group ($P < 0.05$, Fig. 5A–D), and CSI was significantly higher ($P < 0.05$); the mean retinal blood flow density, CVI, and CVV were significantly higher in the EA and EA + Y27632 groups compared with the LIM group, and the differences were statistically significant ($P < 0.05$), and CSI was significantly lower ($P < 0.05$). It indicates that after 4 weeks of modeling, EA can effectively increase retinal and choroidal blood flow density, increase retinal blood supply.

3.5. Effects of EA on the extracellular microenvironment of LIM Guinea pig retina

After 2 and 4 weeks of modeling, the retinas of guinea pigs in each group were extracted for the determination of SOD, GSH, CAT,

Table 3
Ocular refraction difference before and after modeling in each group of guinea pigs (D) (Mean ± SD).

	0w	2w	4w
NC	5.21 ± 1.67	3.17 ± 0.13	1.55 ± 1.45
LIM	5.34 ± 1.82	−3.07 ± 0.87*	−4.83 ± 0.42*
EA	5.13 ± 0.65	−1.19 ± 0.32#	−2.17 ± 0.72#
SHAM	5.04 ± 2.11	−3.68 ± 0.95	−4.21 ± 2.22
EA + Y27632	5.05 ± 1.77	−1.00 ± 0.54#	−2.00 ± 0.20#

Note: #$P < 0.05$, compared with LIM group; *$P < 0.05$ LIM group compared with NC group. (n = 10).

Table 4
Axial Length difference before and after modelling in each group of guinea pigs (mm)(Mean ± SD).

	0w	2w	4w
NC	7.77 ± 0.06	8.02 ± 0.04	8.18 ± 0.02
LIM	7.78 ± 0.06	8.18 ± 0.03*	8.37 ± 0.05*
EA	7.76 ± 0.08	8.10 ± 0.02#	8.24 ± 0.03#
SHAM	7.79 ± 0.05	8.21 ± 0.03	8.34 ± 0.06
EA + Y27632	7.80 ± 0.06	8.08 ± 0.04#	8.21 ± 0.04#

Note: #$P < 0.05$, compared with LIM group; *$P < 0.05$ LIM group compared with NC group. (n = 10).

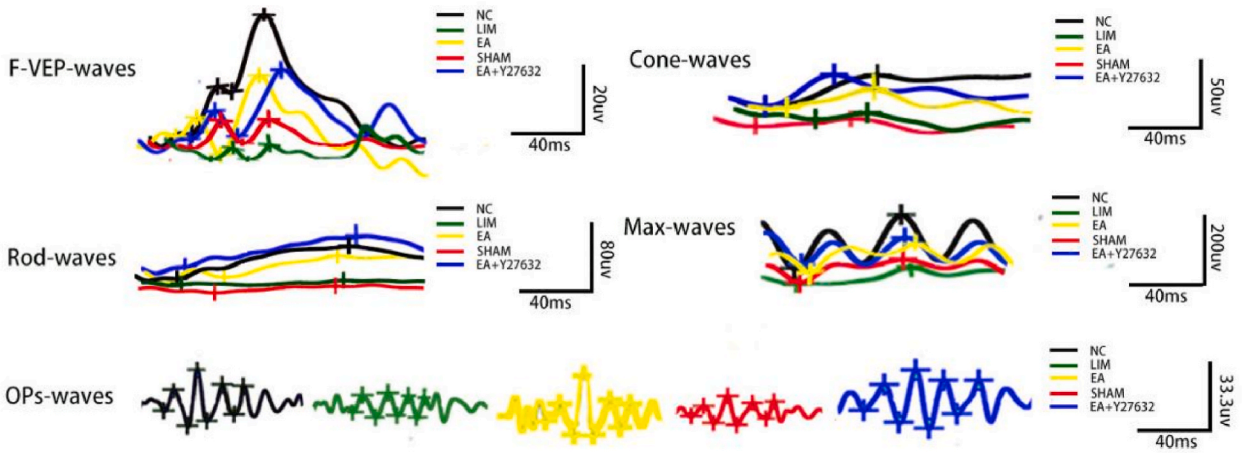

Fig. 3. After 4 weeks of modeling, F-ERG and F-VEP examinations of the retina of the guinea pigs in each group. NC: Normal control; LIM: Lens-induced myopia; EA: Electroacupuncture; SHAM: Sham acupoint.

MDA, and T-AOC contents. The results showed that at the same time point, the SOD, GSH, CAT, and T-AOC contents of the LIM group were lower than those of the NC group, and the MDA contents were higher than those of the NC group (Fig. 6 A-E, $P < 0.05$); the SOD, GSH, CAT, and T-AOC contents of the EA and EA + Y27632 groups were higher than those of the LIM group, and the MDA contents were lower than those of the LIM group. It showed that EA could improve the antioxidant capacity of the retina and delay the development of myopia in LIM guinea pigs.

*3.6. Effect of EA on the expressions of **RhoA**、**ROCK2**、**MLC**、collagenI、MMP-2、TIMP-2 and α-SMA in retina*

The qPCR results showed that at the same time point, the expression of the genes of RhoA, ROCK2, MLC, Collagen I, MMP-2, TIMP-2, and α-SMA were higher in the LIM group than in the NC group (Fig. 7 A-G, $P < 0.05$). The expression levels of RhoA, ROCK2, MLC, Collagen I, MMP-2, TIMP-2, and α-SMA in EA and EA + Y27632 groups were lower than those in the LIM group. Meanwhile, the levels of related proteins were consistent with the trend of gene expression levels (Fig. 8 A-B, Supplementary material S1). In addition, p-MLC/MLC levels were also elevated, indicating that the RhoA/ROCK2 signaling pathway was activated after myopia induction, and the levels of related marker molecules were elevated, which were reduced after EA intervention.

3.7. H&E staining

To investigate the effect of EA on retinal histomorphology, we performed H&E staining after 2 and 4 weeks of treatment in each group (Fig. 9A–C). The results of HE staining showed that, after 2 and 4 weeks of modeling, in the NC group, the boundaries of retinal tissue were obvious, the structure was clear and complete, the arrangement was regular, no edema and abnormal changes were observed, and no abnormal changes were observed in cell structure. In LIM and SHAM groups, there were abnormal changes in the morphology and structure of retinal tissue layers, thinning of retina, the thickness of the inner nuclear layer (INL) and outer nuclear layer (ONL) and the number of cells were reduced. irregular arrangement, significantly reduced number of ganglion cells, and abnormal changes such as cell edema. There were no obvious abnormalities in the morphology and structure of retinal tissue in EA and EA + Y27632 groups, which was close to that in NC group, the cells in each layer were arranged more neatly, the number of cells was not significantly reduced, and no abnormal changes such as cell edema were observed.

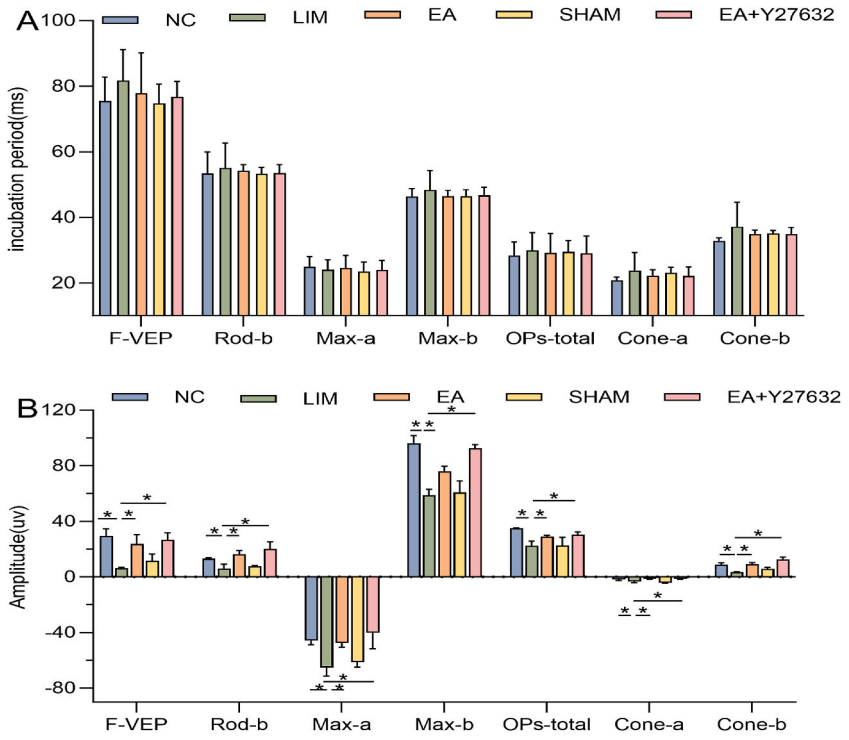

Fig. 4. F-ERG and F-VEP examinations after 4 weeks of modeling.The incubation (A) and peak (B) changes of F-VEP P2 and F-ERG in the retina of guinea pigs in each group.*$P < 0.05$. NC: Normal control; LIM: Lens-induced myopia; EA: Electroacupuncture; SHAM: Sham acupoint. Error bars denote SD. (n = 8).

4. Discussion

In this study, we observed that electroacupuncture effectively reduced myopic refraction and axial elongation, improved retinal function and fundus blood flow, and delayed the progression of myopia in LIM guinea pigs, which is consistent with previous findings [24–26]. However, the precise molecular mechanisms underlying the delay in myopia development by electroacupuncture remain incompletely understood. Therefore, we further investigated the potential involvement of the RhoA/ROCK2 signaling pathway.

Oxidative stress (OS) is a physiological response triggered by endogenous or exogenous factors, disrupting the normal metabolic activities of organs and causing an imbalance between oxidation and antioxidant effects [27].

OS serves as a crucial mechanism underlying the development of myopia. Research has revealed that reactive oxygen species (ROS) and reactive nitrogen species (RNS) can accumulate in the retina and choroid due to various reasons, leading to lipid peroxidation and excessive production of MDA. Consequently, the regulatory mechanism for proper eyeball growth is impaired, resulting in excessive elongation of the ocular axis and subsequent myopia [28]. In order to maintain redox homeostasis within the body, an antioxidant system exists. The system comprises both enzymatic and non-enzymatic antioxidant [29], with examples including CAT, SOD, GSH, vitamin C, transferrin, N-acetylcysteine, among others. ROS not only causes cellular damage through polyunsaturated fatty acid peroxidation but also via decomposition products of lipid hydroperoxides. The activity levels of CAT and SOD indirectly reflect the body's ability to eliminate ROS, while MDA levels indicate the severity of ROS induced cell damage. GSH plays a pivotal role as a non-enzymatic antioxidant within the body by removing ROS, detoxifying substances, promoting iron absorption, and facilitating normal cell development. The quantity of GSH serves as an important factor in assessing overall antioxidant capacity within the body. In this study conducted on LIM guinea pigs after 2 weeks and 4 weeks of modeling respectively, it was observed that retinal MDA content increased while SOD, GSH, CAT, and T-AOC content decreased, indicating that these animals experienced heightened oxidative stress with reduced antioxidant capacity due to ROS attack on their cells. However, EA treatment effectively enhanced retinal antioxidant capacity.

RhoA, a member of the GTPase small family, plays a crucial role in regulating the actin cytoskeleton and exerts significant influence on various fundamental cellular processes including cell proliferation, apoptosis, migration, adhesion, and contraction [30]. Moreover, it also impacts vascular and tissue permeability as well as stress fiber formation. ROCK2 protein serves as the primary downstream target effector of RhoA and is prominently expressed in ocular tissues [31]. The functionality of ROCK2 relies on Myosin light chain (MLC) phosphorylation. In vitro studies have demonstrated that reactive oxygen species can activate the RhoA/ROCK pathway [32]. Oxidative stress triggers ROCK activation which subsequently leads to the activation of extracellular signal-regulated kinase (ERK), mitogen-activated protein kinase (MAPK), etc. This cascade ultimately induces fibrosis and ECM remodeling while regulating downstream gene expression [33]. Y-27632 has been identified as an effective inhibitor of ROCK that specifically targets its

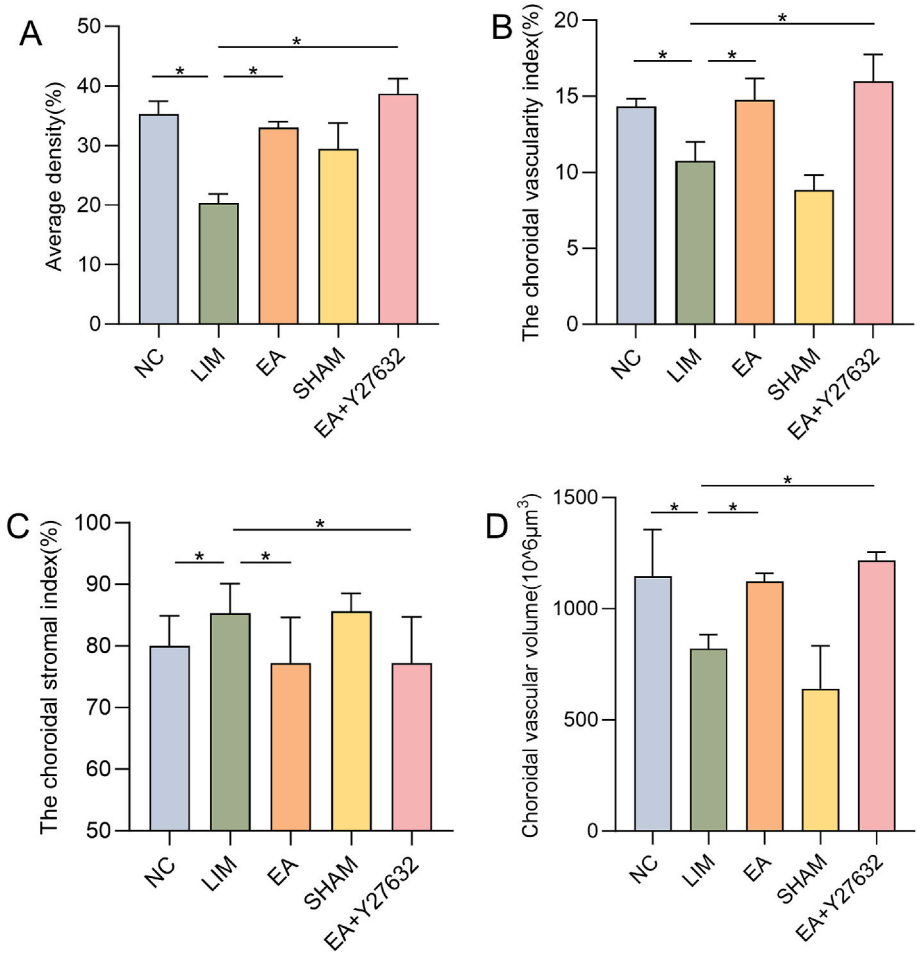

Fig. 5. Average retinal blood flow density(A), CVI(B), CSI(C), and CVV(D) in each group after 4 weeks of modeling × $P < 0.05$ NC: Normal control; LIM: Lens-induced myopia; EA: Electroacupuncture; SHAM: Sham acupoint. Error bars denote SD. (n = 4).

ATP-dependent kinase domain without iso-selectivity, thus equally inhibiting both ROCK1 and ROCK2. Following myopia induction, retinal antioxidant capacity decreases while oxidative stress levels increase along with increased expression of factors related to the RhoA/ROCK pathway activation. However, after both EA intervention and Y-27632 intervention are implemented, inhibition of the RhoA/ROCK pathway occurs resulting in delayed myopia progression.

The extracellular matrix (ECM) is crucial for cell survival and maintaining tissue homeostasis and function. Matrix metalloproteinases (MMPs) are responsible for ECM degradation, while tissue inhibitors of metalloproteinases (TIMPs) inhibit MMP activity, thus ensuring a balance between ECM synthesis and degradation. Tissue ischemia and hypoxia can lead to oxidative stress, disrupt the ECM microenvironment, and affect the MMP/TIMP ratio. Activation of the Rho/ROCK signaling pathway promotes the synthesis of fibritin, laminin, collagen fibers, and hyaluronic acid in the ECM [34]. It also regulates MMP and TIMP expression by controlling downstream gene expression [34,35], leading to an imbalance in MMP/TIMP ratio that affects ECM remodeling and contributes to myopia development. In this study, we observed activation of the Rho/ROCK signaling pathway in the retina of LIM guinea pigs along with an imbalanced MMP/TIMP ratio characterized by increased levels of MMP-2 and TIMP-2 expression. The upregulation of TIMP-2 may be a compensatory response to elevated levels of MMP-2 expression. Electroacupuncture intervention effectively inhibits the RhoA/ROCK signaling pathway and maintains a balanced MMP/TIMP ratio.

ECM remodeling facilitates fibroblast differentiation into myofibroblasts [36]. Myofibroblasts interact with the extracellular matrix through the fibronectin linkage complex and may participate in the regulation of extracellular matrix synthesis and degradation. α-SMA is a cytoskeletal protein expressed in myofibroblasts that serves as their main contractile structure. It plays critical roles in tissue fibrosis, wound healing, and scar formation [37]. The increased expression of Collagen I and α-SMA in the retina after myopia induction suggests that more fibroblasts differentiate into myofibroblasts and ECM remodeling occurs. This finding is consistent with previous research. Li et al. [38] discovered that as myopia increased, the levels of Collagen I and α-SMA in the choroidal membrane also increased, promoting the development of myopia. Hu et al. [39] observed that levels of Collagen I and α-SMA in scleral tissue from rats with elevated intraocular pressure were elevated, resulting in increased scleral hardness. Bao et al. [40] demonstrated that myopia induction could upregulate MMP2, Collagen I, and α-SMA expressions, disrupting the retinal microenvironment in myopic guinea pigs.

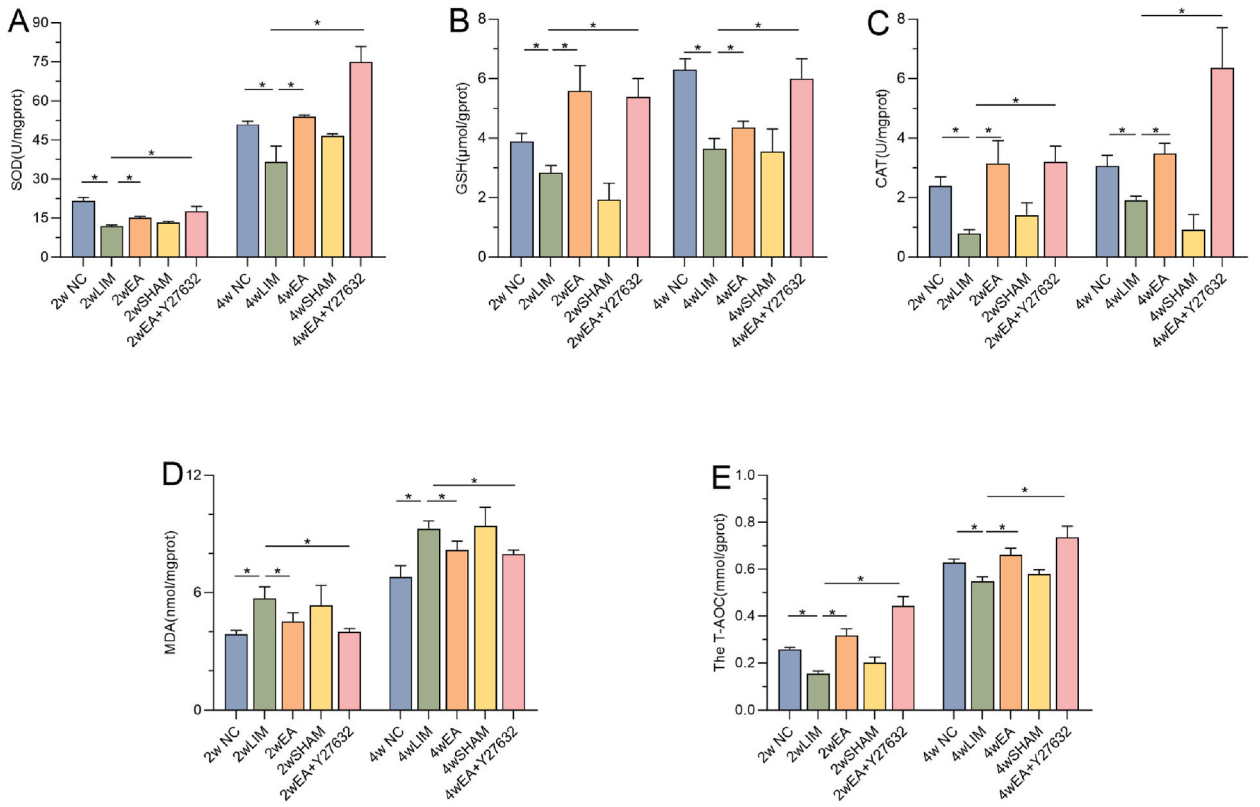

Fig. 6. Measurements of SOD, GSH, CAT, MDA, and T-AOC content. SOD, GSH, CAT, MDA, and T-AOC levels of the retinas in guinea pigs from each group after 2 and 4 weeks of modeling.*$P < 0.05$. NC: Normal control; LIM: Lens-induced myopia; EA: Electroacupuncture; SHAM: Sham acupoint. Error bars denote SD. (n = 4).

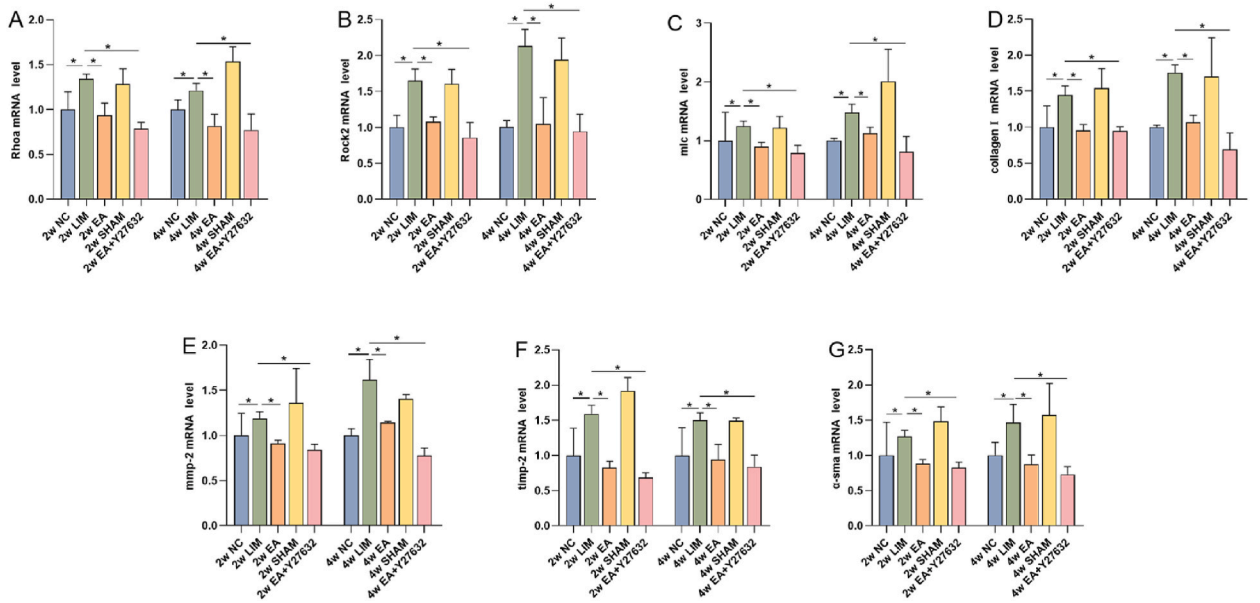

Fig. 7. Determination of mRNA levels. The mRNA expression levels of Rhoa (A), Rock2(B), mlc (C), collagen I(D), mmp-2(E), timp-2(F) and α-sma (G) genes in the retinas of the guinea pigs in each groups were detected by qPCR. *$P < 0.05$, NC: Normal control; LIM: Lens-induced myopia; EA: Electroacupuncture; SHAM: Sham acupoint. Error bars denote SD. (n = 3).

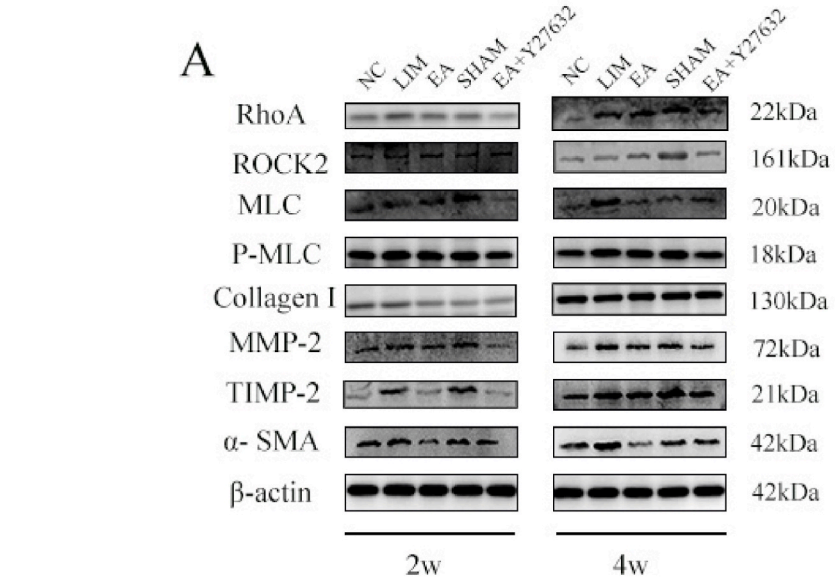

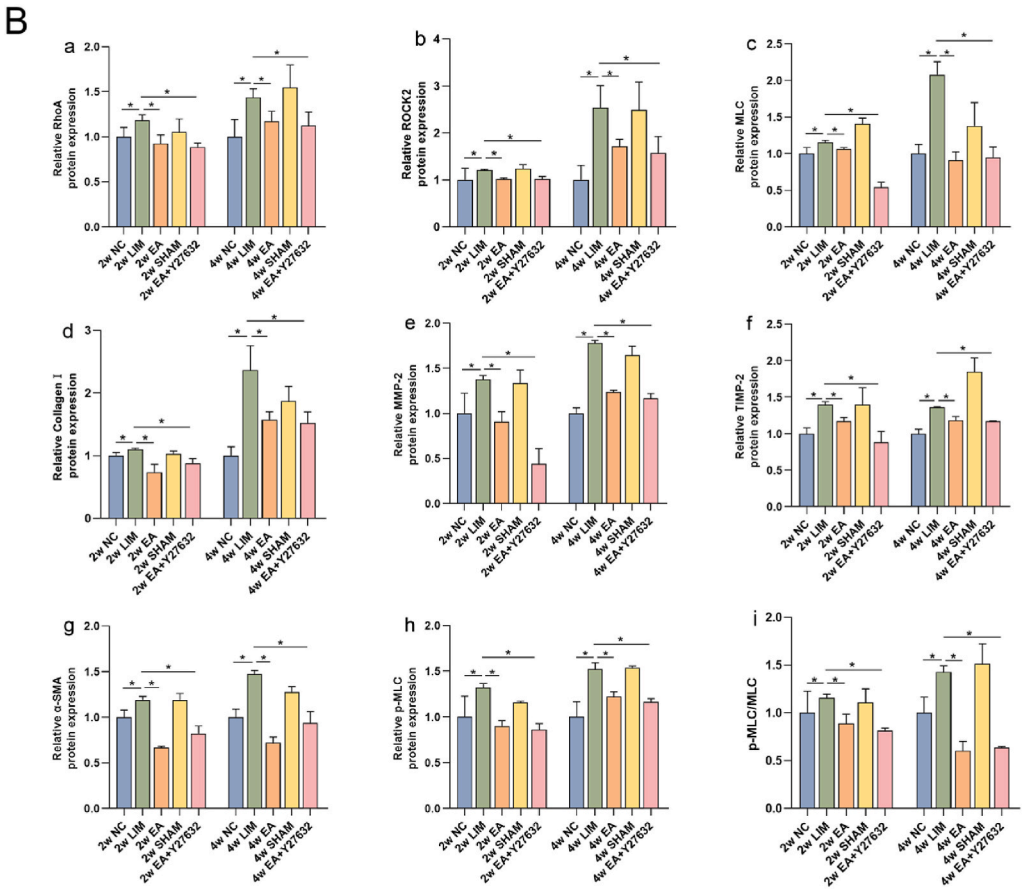

(caption on next page)

Fig. 8. Western blot analysis(A, B). Relative levels of RhoA (a), ROCK2 (b), MLC (c), Collagen I (d), MMP-2 (e), TIMP-2 (f), α-SMA (g), p-MLC (h), and p-MLC/MLC (i) proteins in guinea pigs from each group after 2 and 4 weeks of modeling. Fig. 8 shows a representative of multiple repeated experiments. *P < 0.05NC: Normal control; LIM: Lens-induced myopia; EA: Electroacupuncture; SHAM: Sham acupoint. Error bars denote SD. (n = 4) The uncropped image in Fig. 8A can be found in Supplementary Material S1.

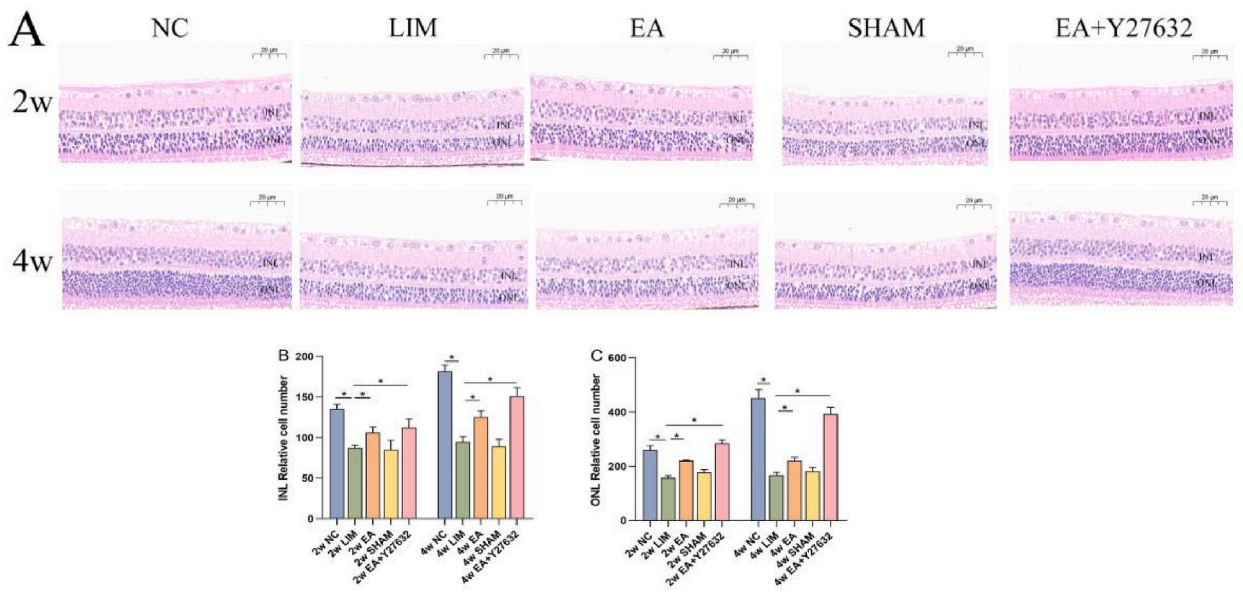

Fig. 9. Histologic morphology of retina after 4 weeks of different treatments. B:quantitative map of INL cell counts; C: quantitative map of ONL cell counts. NC: Normal control; LIM: Lens-induced myopia; EA: Electroacupuncture; SHAM: Sham acupoint. Error bars denote SD. (n = 3).

The expression of Collagen I and α-SMA decreased after EA intervention, indicating that EA attenuates transdifferentiation of myofibroblasts and slows myopia progression.

As one of the most metabolically active tissues within human anatomy, the retina requires ample blood circulation to provide nutrients and oxygen while removing metabolic waste for normal visual function [41,42]. The retina possesses two blood supply systems: the central retinal artery system supplies its inner layer while the choroidal vascular system supplies its outer layer [43]. Previous studies have shown a tendency towards reduced fundus retinal blood flow among patients with myopia. Ye et al. [44] found a significant reduction in deep retinal capillary plexus among individuals with pathological myopia. Li et al. [45] used OCTA to compare the retinal blood vessels of patients with different degrees of myopia and found that the density of large blood vessels and microvessels in the shallow retina of highly myopia patients was significantly reduced. These studies suggest that retinal hemodynamic changes affect the occurrence and development of myopia. Studies have shown that the RhoA/ROCK2 signaling pathway regulates the contraction of intraocular vascular smooth muscle and is involved in the regulation of intraocular blood flow, endothelial barrier [46], cell migration, and angiogenesis [47]. In this study, we found that the retinal blood flow density, CVI, and CVV of LIM guinea pigs were reduced. The local oxygen supply of the retina was insufficient, which activated the RhoA/ROCK signaling pathway. RhoA/ROCK and its downstream genes caused changes in retinal structure and function by affecting retinal nerve and blood vessel function and ECM remodeling. Leading to the occurrence and development of myopia. We hypothesized that the RhoA/ROCK2 signaling pathway is involved in the regulation of retinal function in myopic guinea pigs and is the key mechanism affecting retinal function in LIM guinea pigs.

ERG and F-VEP can objectively reflect the process of visual information from photoreceptor cells receiving external light stimulation to transmitting bioelectrical information to the visual center and are widely used in visual function evaluation [48,49]. F-ERG reflects the functions of the first and second-order neurons in the retina, which are mainly composed of a wave, b wave, and Ops wave. a waves originate from photoreceptor cells, and b waves reflect the function of bipolar cells or muller cells. OPs waves originate from the inner layer of the retina and reflect the feedback mechanism from amacrine cells to bipolar cells, interreticular cells, horizontal cells, and other amacrine cells. EA stimulation points can affect the latency and peak of F-ERG waves. Duan et al. [50] found that EA stimulation at Hegu point can advance the latency of b wave and increase the peak values of a wave and b wave, suggesting that acupuncture may cause the release of retinal neurotransmitters to change the distribution of K+, thus affecting the latency and peak values of a wave and b wave of ERG. OPs originates from the inner nuclear layer of the retina and is closely related to the function of the inner retinal layer, which is a sensitive indicator reflecting the retinal blood circulation. In this study, after 4 weeks of modeling, the peaks of a-wave, b-wave, and OPs-total in LIM guinea pigs were significantly reduced compared with NC, indicating that LIM guinea pigs may have dysfunction of photoreceptor cells, bipolar cells and müller cells. SS-OCTA examination showed that retinal blood flow density, CVV, and CVI decreased, indicating reduced retinal blood supply. After the intervention of EA, the peak values of a and b of

dark adaptation and light adaptation significantly increased, the peak value of OPs-total significantly increased and reached the normal level, and the retinal blood flow density, CVV, and CVI increased, indicating that EA can effectively improve the function of the inner and outer layers of retina, improve the eye blood circulation, and thus relieve the spasm of the smooth muscle of the blood vessel wall and restore the vasomotor function. Increases blood supply to the eyes.

5. Conclusion

In summary, we confirmed that experimental myopia can cause reduced retinal blood supply, increased oxidative damage, activation of the RhoA/ROCK2 signaling pathway, imbalance in the ratio of MMP and TIMP, elevated expression of Collagen I and α-SMA, and ECM remodeling, which leads to retinal dysfunction and promotes the development of myopia. EA can reduce the risk of myopia by increasing retinal blood flow, ameliorating retinal oxidative stress, and inhibiting the RhoA/ROCK2 signaling pathway. ROCK signaling pathway, regulating the expression of genes downstream of the RhoA/ROCK2 signaling pathway, affecting retinal ECM remodeling, alleviating retinal dysfunction, and delaying the development of myopia. Our study contributes to an in-depth understanding of the pathogenesis of myopia, and can also provide a theoretical basis for optimising acupuncture protocols and new insights into the treatment of myopia by EA.

Ethics statement

The study was approved by the Experimental Animal Ethics Review Committee of the Affiliated Hospital of Shandong University of Traditional Chinese Medicine (Approval number: AWE-2022-055) and followed the Association for Research in Vision and Ophthalmology (ARVO) guidelines for animal use in vision research.

Funding

This study was supported by grants from the National Natural Science Foundation of China (82104937), the Program of Traditional Chinese Medicine Science and Technology Project of Shandong Province (No. M-2023010); the Program of Traditional Chinese Medicine Science and Technology Project of Shandong Province (No.202207020876, 2019WS572); the National key research and development program of China (2021YFC2702103, 2021YFC2702100 and 2021YFC2702104).

Data availability statement

The data will be made available on request.

CRediT authorship contribution statement

Yijie Liu: Writing – original draft, Data curation. **Qi Hao:** Data curation. **Xiuzhen Lu:** Funding acquisition, Conceptualization. **Pubo Wang:** Data curation. **Dadong Guo:** Funding acquisition, Data curation, Conceptualization. **Xiuyan Zhang:** Funding acquisition. **Xuemei Pan:** Funding acquisition. **Qiuxin Wu:** Writing – review & editing, Writing – original draft, Project administration, Funding acquisition, Data curation, Conceptualization. **Hongsheng Bi:** Project administration, Methodology, Funding acquisition.

Declaration of competing interest

The authors declare the following financial interests/personal relationships which may be considered as potential competing interests: Qinxin wu reports financial support was provided by the National Natural Science Foundation of China. Qinxin wu reports financial support was provided by the Program of Traditional Chinese Medicine Science and Technology Project of Shandong Province. Qinxin wu reports financial support was provided by the Program of Traditional Chinese Medicine Science and Technology Project of Shandong Province. Qinxin wu reports financial support was provided by the National key research and development program of China. If there are other authors, they declare that they have no known competing financial interests or personal relationships that could have appeared to influence the work reported in this paper.

Acknowledgements

The authors thank the members of their laboratory and their collaborators for their support.

Abbreviations

EA	electroacupuncture
NC	Normal control
LIM	lens-induced myopia
SHAM	SHAM acupoint
AL	axial length

CVI	choroidal vascular index
T-AOC	total antioxidant capacity
CAT	catalase
GSH	glutathione
SOD	superoxide dismutase
MDA	malondialdehyde
H&E	hematoxylin and eosin
qPCR	real-time quantitative polymerase chain reaction
RPE	retinal pigment epithelium
ECM	extracellular matrix
D	diopter
F-VEP	Flash visual evoked potential
F-ERG	flash electroretinography
SS-OCTA	Swept-Source Optical Coherence Tomography Angiography
CVV	Choroidal vascular volume
CSI	choroidal stromal index
PMSF	phenylmethylsulfonyl fluoride
RIPA	radioimmunoprecipitation assay buffer lysate
PVDF	polyvinylidene difluoride
TIMP-2	tissue inhibitor of metalloproteinase-2
MMP-2	matrix metalloproteinase 2
ECL	enhanced chemiluminescence
INL	inner nuclear layer
ONL	outer nuclear layer
OS	Oxidative stress
ROS	reactive oxygen species
RNS	reactive nitrogen species
MLC	Myosin light chain
ERK	extracellular signal-regulated kinase
MAPK	mitogen-activated protein kinase

Appendix A. Supplementary data

Supplementary data to this article can be found online at https://doi.org/10.1016/j.heliyon.2024.e35750.

References

[1] B.A. Holden, T.R. Fricke, D.A. Wilson, M. Jong, K.S. Naidoo, P. Sankaridurg, T.Y. Wong, T.J. Naduvilath, S. Resnikoff, Global prevalence of myopia and high myopia and temporal trends from 2000 through 2050, Ophthalmology 123 (5) (2016) 1036–1042.

[2] L. Dong, Y.K. Kang, Y. Li, W.B. Wei, J.B. Jonas, Prevalence and time trends of myopia in children and adolescents in China: a systemic review and meta-analysis, Retina 40 (3) (2020) 399–411.

[3] Y. Huang, X. Chen, J. Zhuang, K. Yu, The role of retinal dysfunction in myopia development, Cell. Mol. Neurobiol. 43 (5) (2023) 1905–1930.

[4] L. Su, Y.S. Ji, N. Tong, D. Sarraf, X. He, X. Sun, X. Xu, S.R. Sadda, Quantitative assessment of the retinal microvasculature and choriocapillaris in myopic patients using swept-source optical coherence tomography angiography, Graefes Arch. Clin. Exp. Ophthalmol. 258 (6) (2020) 1173–1180.

[5] Y. Yuan, M. Li, C.H. To, T.C. Lam, P. Wang, Y. Yu, Q. Chen, X. Hu, B. Ke, The role of the RhoA/ROCK signaling pathway in mechanical strain-induced scleral myofibroblast differentiation, Invest. Ophthalmol. Vis. Sci. 59 (8) (2018) 3619–3629.

[6] J.J. Walline, K.B. Lindsley, S.S. Vedula, S.A. Cotter, D.O. Mutti, S.M. Ng, J.D. Twelker, Interventions to slow progression of myopia in children, Cochrane Database Syst. Rev. 1 (2020) CD004916.

[7] H. Wu, W. Chen, F. Zhao, Q. Zhou, P.S. Reinach, L. Deng, L. Ma, S. Luo, N. Srinivasalu, M. Pan, Y. Hu, X. Pei, J. Sun, R. Ren, Y. Xiong, Z. Zhou, S. Zhang, G. Tian, J. Fang, L. Zhang, J. Lang, D. Wu, C. Zeng, J. Qu, X. Zhou, Scleral hypoxia is a target for myopia control, Proc. Natl. Acad. Sci. U. S. A. 115 (30) (2018) E7091–E7100.

[8] Q. Wei, T. Zhang, J. Fan, R. Jiang, Q. Chang, J. Hong, G. Xu, Pathological myopia-induced antioxidative proteins in the vitreous humor, Ann. Transl. Med. 8 (5) (2020) 193.

[9] G. Loirand, P. Guérin, P. Pacaud, Rho kinases in cardiovascular physiology and pathophysiology, Circ. Res. 98 (3) (2006) 322–334.

[10] Y. Xu, K. Cui, J. Li, X. Tang, J. Lin, X. Lu, R. Huang, B. Yang, Y. Shi, D. Ye, J. Huang, S. Yu, X. Liang, Melatonin attenuates choroidal neovascularization by regulating macrophage/microglia polarization via inhibition of RhoA/ROCK signaling pathway, J. Pineal Res. 69 (1) (2020) e12660.

[11] H. Tanihara, T. Inoue, T. Yamamoto, Y. Kuwayama, H. Abe, H. Suganami, M. Araie, K-115 Clinical Study Group, Intra-ocular pressure-lowering effects of a Rho kinase inhibitor, ripasudil (K-115), over 24 hours in primary open-angle glaucoma and ocular hypertension: a randomized, open-label, crossover study, Acta Ophthalmol. 93 (4) (2015) e254–e260.

[12] Y. Ohta, S. Takaseki, T. Yoshitomi, Effects of ripasudil hydrochloride hydrate (K-115), a Rho-kinase inhibitor, on ocular blood flow and ciliary artery smooth muscle contraction in rabbits, Jpn. J. Ophthalmol. 61 (5) (2017) 423–432.

[13] S. Nakabayashi, M. Kawai, T. Yoshioka, Y.S. Song, T. Tani, A. Yoshida, T. Nagaoka, Effect of intravitreal Rho kinase inhibitor ripasudil (K-115) on feline retinal microcirculation, Exp. Eye Res. 139 (2015) 132–135.

[14] X. Fang, M. Ueno, T. Yamashita, Y. Ikuno, RhoA activation and effect of Rho-kinase inhibitor in the development of retinal neovascularization in a mouse model of oxygen-induced retinopathy, Curr. Eye Res. 36 (11) (2011) 1028–1036.

[15] Y. Hata, M. Miura, S. Nakao, S. Kawahara, T. Kita, T. Ishibashi, Antiangiogenic properties of fasudil, a potent Rho-Kinase inhibitor, Jpn. J. Ophthalmol. 52 (1) (2008) 16–23.
[16] M. Yamaguchi, S. Nakao, R. Arita, Y. Kaizu, M. Arima, Y. Zhou, T. Kita, S. Yoshida, K. Kimura, T. Isobe, Y. Kaneko, K.H. Sonoda, T. Ishibashi, Vascular normalization by ROCK inhibitor: therapeutic potential of ripasudil (K-115) eye drop in retinal angiogenesis and hypoxia, Invest. Ophthalmol. Vis. Sci. 57 (4) (2016) 2264–2276.
[17] I.V. Hove, E. Lefevere, L. Moons, ROCK inhibition as a novel potential strategy for axonal regeneration in optic neuropathies, Neural Regen Res 10 (12) (2015) 1949–1950.
[18] S. Van de Velde, L. De Groef, I. Stalmans, L. Moons, I. Van Hove, Towards axonal regeneration and neuroprotection in glaucoma: Rho kinase inhibitors as promising therapeutics, Prog. Neurobiol. 131 (2015) 105–119.
[19] R.R. Li, X.B. Hua, H.L. Zhou, HuYL. SongDL, Development of acupuncture point atlas for Guinea pig, Shanghai Journal of Acupuncture and Moxibustion (2) (1992) 28–30.
[20] S.S. Wu, H.X. Wei, B. Guo, X.W. Yin, D.Z. Liu, D.D. Guo, H.S. Bi, Effect of electroacupuncture on expression of epidermal growth factor and its receptor in ciliary muscle of lens-induced myopic Guinea pigs, Recent Advances in Ophthalmology 40 (4) (2020) 318–322.
[21] D.L. McCulloch, M.F. Marmor, M.G. Brigell, R. Hamilton, G.E. Holder, R. Tzekov, M. Bach, ISCEV Standard for full-field clinical electroretinography (2015 update), Doc. Ophthalmol. 130 (1) (2015) 1–12.
[22] R. Agrawal, P. Gupta, K.A. Tan, C.M. Cheung, T.Y. Wong, C.Y. Cheng, Choroidal vascularity index as a measure of vascular status of the choroid: measurements in healthy eyes from a population-based study, Sci. Rep. 6 (2016) 21090.
[23] K.J. Livak, T.D. Schmittgen, Analysis of relative gene expres-sion data using real-time quantitative PCR and the 2−??CT method, Methods 25 (2001) 402–408.
[24] S. Huang, D. Huang, J. Zhao, L. Chen, Electroacupuncture promotes axonal regeneration in rats with focal cerebral ischemia through the downregulation of Nogo-A/NgR/RhoA/ROCK signaling, Exp. Ther. Med. 14 (2) (2017) 905–912.
[25] H. Tao, S.F. Liu, M. Ling, Study on the mechanism of vascular endothelial protection in hyperlipidaemia model rats by acupuncture based on Rho/ROCK signalling pathway, Journal of Basic Chinese Medicine 25 (8) (2019) 1134–1136+1142.
[26] Y. Han, S. Chen, H. Wang, X.M. Peng, Electroacupuncture pretreatment regulates apoptosis of myocardial ischemia-reperfusion injury in rats through RhoA/p38MAPK pathway mediated by miR-133a-5p, Evid Based Complement Alternat Med 2021 (2021) 8827891.
[27] Y.X. Zi, M. Jin, Recent advances on oxidative stress in pathogenesis of high myopia, Recent Advances in Ophthalmology 40 (4) (2020) 388–391.
[28] Z. Zhuang, L. Li, Y. Yu, X. Su, S. Lin, J. Hu, Targeting MicroRNA in myopia: current insights, Exp. Eye Res. 243 (2024) 109905.
[29] N.S. Mashhadi, R. Ghiasvand, G. Askari, M. Hariri, L. Darvishi, M.R. Mofid, Anti-oxidative and anti-inflammatory effects of ginger in health and physical activity: review of current evidence, Int. J. Prev. Med. 4 (Suppl 1) (2013) S36–S42.
[30] G. Loirand, P. Guérin, P. Pacaud, Rho kinases in cardiovascular physiology and pathophysiology, Circ. Res. 98 (3) (2006) 322–334.
[31] G. Loirand, Rho kinases in health and disease: from basic science to translational research, Pharmacol. Rev. 67 (4) (2015) 1074–1095.
[32] L. Jin, Z. Ying, R.C. Webb, Activation of Rho/Rho kinase signaling pathway by reactive oxygen species in rat aorta, Am. J. Physiol. Heart Circ. Physiol. 287 (4) (2004) H1495–H1500.
[33] R. Proietti, A.S. Giordani, C.A. Lorenzo, ROCK (RhoA/Rho kinase) activation in atrial fibrillation: molecular pathways and clinical implications, Curr. Cardiol. Rev. 19 (3) (2023) e171122210986.
[34] H. Ji, H. Tang, H. Lin, J. Mao, L. Gao, J. Liu, T. Wu, Rho/Rock cross-talks with transforming growth factor-β/Smad pathway participates in lung fibroblast-myofibroblast differentiation, Biomed Rep 2 (6) (2014) 787–792.
[35] Y. Xie, T. Song, M. Huo, Y. Zhang, Y.Y. Zhang, Z.H. Ma, N. Wang, J.P. Zhang, L. Chu, Fasudil alleviates hepatic fibrosis in type 1 diabetic rats: involvement of the inflammation and RhoA/ROCK pathway, Eur. Rev. Med. Pharmacol. Sci. 22 (17) (2018) 5665–5677.
[36] H. Wu, W. Chen, F. Zhao, Q. Zhou, P.S. Reinach, L. Deng, L. Ma, S. Luo, N. Srinivasalu, M. Pan, Y. Hu, X. Pei, J. Sun, R. Ren, Y. Xiong, Z. Zhou, S. Zhang, G. Tian, J. Fang, L. Zhang, J. Lang, D. Wu, C. Zeng, J. Qu, X. Zhou, Scleral hypoxia is a target for myopia control, Proc. Natl. Acad. Sci. U. S. A. 115 (30) (2018) E7091–E7100.
[37] N.L. Batenburg, E.L. Thompson, E.A. Hendrickson, X.D. Zhu, Cockayne syndrome group B protein regulates DNA double-strand break repair and checkpoint activation, EMBO J. 34 (10) (2015) 1399–1416.
[38] T. Li, X. Li, Y. Hao, J. Liu, B. Bao, Z. Yang, M. Zhou, H. Wei, R. Zhang, J. Hao, W. Jiang, H. Bi, D. Guo, Inhibitory effect of miR-138-5p on choroidal fibrosis in lens-induced myopia Guinea pigs via suppressing the HIF-1α signaling pathway, Biochem. Pharmacol. 211 (2023) 115517.
[39] D. Hu, J. Jiang, B. Ding, K. Xue, X. Sun, S. Qian, Mechanical strain regulates myofibroblast differentiation of human scleral fibroblasts by YAP, Front. Physiol. 12 (2021) 712509.
[40] B. Bao, J. Liu, T. Li, Z. Yang, G. Wang, J. Xin, H. Bi, D. Guo, Elevated retinal fibrosis in experimental myopia is involved in the activation of the PI3K/AKT/ERK signaling pathway, Arch. Biochem. Biophys. 743 (2023) 109663.
[41] W.S. Foulds, Retinal metabolism and the choroidal circulation, Eye 4 (Pt 2) (1990) ix–x.
[42] Y. Sun, L.E.H. Smith, Retinal vasculature in development and diseases, Annu Rev Vis Sci. 4 (2018) 101–122.
[43] T.H. Williamson, A. Harris, Ocular blood flow measurement, Br. J. Ophthalmol. 78 (12) (1994) 939–945.
[44] J. Ye, M. Wang, M. Shen, S. Huang, A. Xue, J. Lin, Y. Fan, J. Wang, F. Lu, Y. Shao, Deep retinal capillary plexus decreasing correlated with the outer retinal layer alteration and visual acuity impairment in pathological myopia, Invest. Ophthalmol. Vis. Sci. 61 (4) (2020) 45.
[45] M. Li, Y. Yang, H. Jiang, G. Gregori, L. Roisman, F. Zheng, B. Ke, D. Qu, J. Wang, Retinal microvascular network and microcirculation assessments in high myopia, Am. J. Ophthalmol. 174 (2017) 56–67.
[46] L. Claesson-Welsh, E. Dejana, D.M. McDonald, Permeability of the endothelial barrier: identifying and reconciling controversies, Trends Mol. Med. 27 (4) (2021) 314–331.
[47] J. Liu, Y. Wada, M. Katsura, H. Tozawa, N. Erwin, C.M. Kapron, G. Bao, J. Liu, Rho-associated coiled-coil kinase (ROCK) in molecular regulation of angiogenesis, Theranostics 8 (21) (2018) 6053–6069.
[48] T.Y. Xie, Q. Li, X.Y. Chen, Histopathological changes in retinas and F-ERG features of streptozotocin-induced diabetic rats treated with ozone, Int. J. Ophthalmol. 9 (6) (2016) 816–820.
[49] L. Hejsek, J. Ernest, P. Němec, L. Rejmont, K. Manethová, A. Stepanov, P. Rozsíval, Operační řešení u velmi pokročilých rhegmatogenních amocí [Surgical treatment of very advanced rhegmatogenous retinal detachment], Ceska a Slov. Oftalmol. 69 (6) (2013), 248-52. Czech.
[50] J.G. Duan, H.X. Zhou, The effect of different acupoint electrodes on the flash electroretinogram of the rabbit, Chin. Acupunct. Moxibustion 12 (1996) 36–39.